

Internal attack by sulphates in cement pastes and mortars dosed with different levels of pyrite

Ana Paula Brandão Capraro¹ · Vinícius Braga¹ · Marcelo Henrique Farias de Medeiros¹ · Juarez Hoppe Filho² · Mariana O. G. P. Bragança³ · Kleber Franke Portella³ · Isabela Cristina de Oliveira⁴

Received: 6 May 2017 / Accepted: 11 July 2017 / Published online: 15 July 2017
© Springer International Publishing AG 2017

Abstract This study aims to investigate cementitious compound behaviour at early stages (up to 168 days), primarily when dosed with different levels of pyrite. To accomplish this, a study was conducted with cement pastes and mortars contaminated by sulphide. For the cement pastes, four contaminant levels were adopted: with one as a reference value (0%), two as cited by the standards, and one value greater than the set standards. In the mortars, two series were studied, one without contamination and the other with use of an aggregate contaminated naturally by pyrite. Pozzolanic cement was used (65% Portland cement CPV + 35% fly ash) and the materials were submerged in curing compounds for 28 days.

Subsequently, the samples were subjected to two exposure conditions: 1—a wet-dry cycle and 2—immersion in aqueous solution with aeration. To identify the products formed by pyrite oxidation, and the subsequent by-product-based reactions, and cement hydrates, scanning electron microscopy with elemental analysis was used. For the analysis of the mechanical properties, strength tests were performed to test axial compression and tensile strength in bending. Furthermore, monitoring of the dimensional variation in prisms ($2.5 \times 2.5 \times 28.5$) cm³ was performed. In conclusion, we determined that at the exposure times tested, there were signs of sulphide oxidation in the contaminated compounds. It was proven that the higher the degree of pyrite contamination, the higher the relative expansion of the series, which was confirmed by the formation of expansive products identified in the scanning electron microscopy.

✉ Ana Paula Brandão Capraro
anapcapraro@gmail.com

Vinícius Braga
vdasilvabraga@yahoo.com.br

Marcelo Henrique Farias de Medeiros
medeiros.ufpr@gmail.com

Juarez Hoppe Filho
juarez.hoppe@gmail.com

Mariana O. G. P. Bragança
mariana.portella@lactec.org.br

Kleber Franke Portella
portella@lactec.org.br

Isabela Cristina de Oliveira
isabela.oliveira@copel.com

Keywords Internal attack by sulphides · Pyrite · Oxidation · Concrete · Durability

1 Introduction

The concrete structure degradation-mechanisms, attacked internally by sulphates, are caused primarily by the sulphide mineral oxidation phenomenon, which generates expansion and the appearance of cracks, due to the stress caused by crystallization of the new by-products with superior volume to the original [1–3]. Additionally, the products generated by this phenomenon react with the compounds of the hydrated cement, aluminatetri-calcium (C₃A), calcium silicate hydrate (CSH) and calcium hydroxide (Ca(OH)₂), forming new products [4–6].

The expansion mechanism, due to the formation of harmful by-products, from the internal attack by sulphates,

¹ PPGCEC, Universidade Federal do Paraná (UFPR), Curitiba, Brazil

² CCET, Universidade Federal do Oeste da Bahia (UFOB), Barreiras, Brazil

³ LACTEC, Institutos Lactec, Curitiba, Brazil

⁴ COPEL, Companhia Paranaense de Energia Elétrica, Curitiba, Brazil

can be summarized as follows: in the first stages, approximately 200 days, the originating products, such as ettringite, are formed in the voids, pores and interface of the paste-aggregate of cementitious compounds, but without causing internal tensions. Over time, these products begin to fill the voids and pores, depleting the accommodation capacity of the internal structure. Consequently, internal stresses are generated in the material and the formation of cracks and reduction of load bearing capacity occurs [7–9].

The two compounds formed by the oxidation of pyrites (Eq. 1), ferrous sulphate (FeSO_4) and sulphuric acid (H_2SO_4), are water soluble and capable of reacting with hydrated compounds, making possible an internal attack [10]. The main products formed due to the deleterious reactions, between the compounds resulting from the pyrite oxidation process and hydrated compounds of the cement paste, are ettringite ($3\text{CaO}\cdot\text{Al}_2\text{O}_3\cdot3\text{CaSO}_4\cdot32\text{H}_2\text{O}$), gypsum ($\text{CaSO}_4\cdot2\text{H}_2\text{O}$) and thaumasite ($\text{CaSiO}_3\cdot\text{CaCO}_3\cdot\text{CaSO}_4\cdot15\text{H}_2\text{O}$) [1, 2, 4–7].



Among the factors that affect the oxidation mechanism of the sulphides, the alkalinity of the concrete is an influential factor. The pyrite oxidation reaction is favoured under conditions where the hydrogen potential (pH) varies between 12.5 and 13.7, while values greater than 10 cause instability in the sulphide compound [11, 12].

Two major factors that accelerate the chemical modification process of the sulphides present in the rock are the specific surface of the mineral and the chemical composition, more specifically, its iron content. The last one explains the higher oxidation rate of pyrite (FeS) with respect to pyrite (FeS_2). Both factors are related to sulphite oxidation rate and are thus, regulating risk parameters of using aggregates for concrete [12, 13].

The main influencing factors on the oxidation process are oxygen concentration, the presence of moisture, specific sulphide surface, iron content contained in the sulphide, presence of bacterium, ambient temperature, sulphide morphology and pH of the system [7].

Aggregates containing sulphide minerals, such as pyrite, are considered unsuitable for use in concrete structures, since they can cause damage to the durability of structures [14]. However, in large works, it is common that the viability of the enterprise has as an influencing factor. The possibility of extracting aggregates from natural resources existing in their surroundings, since long distances require high transport costs. Thus, this is a key factor in the implementation of a given structure. In addition, aggregates must be considered non-renewable resources; in this way, the use of sand and gravel contaminated by sulphide minerals may become a necessity even for common construction. This context explains the importance of

investigating the degradation mechanisms by internal sulphates further develop ways to mitigate the process through the introduction of new components in concrete dosing, similar to what is currently being done in aggregated alkali reactions [9, 15]. Some documents mentioned below set maximum limits for the contamination of concrete structures by sulphur compounds. There are some recommendations applied via technical means, such as those cited by CEMIG [16]:

- The General German Assembly study of mineral deposits (1960) states that the maximum content of SO_3 should be 1% compared to total aggregate mass;
- The International Committee on Large Dams (1965) study of sulphate and sulphide content must be determined by an analytical chemical method and calculated in terms of equivalent SO_3 . The value cannot exceed 0.5% of the mass of large aggregates used;
- The Portuguese Concrete Regulation of (1971) states that for Portland cement concrete, the following maximum amounts of sulphide in relation to the cement mass are allowed: 0.2% sulphide for concrete with addition of pozzolan, 0.5% for plain concrete, 0.2% for reinforced concrete and 0.05% for pre-stressed concrete. For concrete with blast furnace cement, the presence of sulphide in the aggregate is not tolerated;
- The French standard, AFNOR NF P 18-540 (1997), establishes, for hydraulic concrete, the maximum sulphur limit expressed in SO_3 , 1% relative to the added mass or if the aggregate is contaminated with pyrite, it adopts the value of 0.75% pyrite in relation to the aggregate mass [17];
- The Brazilian standard indicates that aggregates containing sulphates can be used, provided that the total content, expressed as SO_4^{2-} , does not exceed 0.1% in mass. If the limit is exceeded, the aggregates may also be used, provided that the content of SO_4^{2-} , brought to the concrete by all its components (water, aggregates, cement, chemical additives and additions), does not exceed 0.2% of the total mass [18];
- The American Concrete Institute sets the limit of 0.5% SO_3 content in the total aggregated mass [19].

According to the cited information, technical standards and recommendations, it was found that, for the most part, the contents are limited to the total mass of aggregates, except for the Portuguese concrete regulation, which sets values in relation to the cement mass. This information is plausible, since the mechanism is triggered by chemical reactions between the materials contaminated by the sulphur and hydrated cement products. This way, the content limitation with respect to the cement mass was directly linked to the occurrence or severity of the attack by internal sulphates.

Due to the levels recommended by normalizations, this study sets to evaluate the microstructures and mechanical changes of cement pastes and mortars, contaminated by sulphides, for at least 168 days. The contamination of the pastes was artificial, being made by the addition of pyrite content in the compositions (0.0, 0.5, 1.0, 5.0% SO₃). On the mortar, an aggregate with natural pyrite contamination was used.

2 Materials and methods

2.1 Materials

The materials used in the study were the CP V-ARI cement, fly ash, pyrite and limestone fillers. Since the study has an element of chemical analysis, it was opted that the cementitious system composition be made in a laboratory, fixing CP V-ARI replacement content of fly ash by 35%. This is accordance with the maximum established by the Brazilian standard [20], determining a range of values to classify the composition as a type CP IV cement (pozzolan cement).

The CP V-ARI cement employed has a density of 3.13 g/cm³ and specific BET area of 1.07 m²/g. Fly ash comes from the combustion of coal mined in the Brazil and presented specific mass of 1.95 g/cm³, and specific BET area of 1.09 m²/g. Table 1 presents the results of the chemical analysis by X-ray fluorescence of the Portland cement and the fly ash.

Pyrite was used as a contaminant to be added to the cement pastes. The material comes from the Paraná region (Brazil) and is a residue of the coal beneficiation process. Pyrite has density of 4.95 g/cm³, and after grinding, was classified as a passing material through a sieve with a mesh aperture of 2.4 mm.

The limestone filler was used for mass compensation in the cement pastes. As in each group of pastes, the addition of contaminated material was made; the filler was used to ensure all pastes possessed the same proportions, considering this material is inert. The density of the carbonatic material is 2.84 g/cm³.

In the mortars study, two different fine aggregates were employed without using pyrite as a contaminant:

- *Reference mix proportion* Natural sand from the Paraná region (Brazil) with density equal to 2.38 g/cm³, classified as thin by the Brazilian standard [21].
- *Contaminated mix proportion* Sand originated from crushed rock of the Paraná region (Brazil), containing mineral sulphide (pyrite) in its partial composition. The specific mass of the material is equal to 2.96 g/cm³ and it is classified as average by the Brazilian standard [21]. The chemical composition of the material, carried out by X-ray fluorescence is presented in Table 2 [22].

From the selected materials, cement pastes were prepared with and without the addition of pyrite, and mortars with natural aggregate and contaminated, for evaluation of the deterioration mechanisms caused by the reaction of cement hydrates with sulphate ions originating from the oxidation of the sulphide mineral.

2.1.1 Cement pastes

For contamination of the cement pastes, four SO₃ levels were adopted, one of them as a reference (0% contamination), two by the recommended standards, 0.5 and 1.0%, and one above recommended standards (5.0% content). In this study, the used material was pyrite (FeS₂), and thus, the SO₃ concentration was converted to proportional mass values of sulphur in pyrite, as by the results shown in Table 3.

As described above, most of the standards [17–19] limit the level of use of materials containing sulphides in relation to the total weight of the aggregates. As no aggregate was used in the cement paste, for the application of the recommended levels, a mix proportion of the concrete base was adopted, to then determine the level regarding the cement mass.

The used concrete mix was: 1.0 kg cement, 2.7 kg fine aggregate, 2.7 kg coarse aggregate and 0.6 kg water. The choice of this ratio results from the application of an average trace on conventional concrete implementation in a

Table 1 Chemical analysis by X-ray fluorescence, CP V-ARI cement and fly ash

Materials	Chemical composition (%)										
	CaO	SiO ₂	Al ₂ O ₃	Fe ₂ O ₃	SO ₃	MgO	K ₂ O	Na ₂ O	TiO ₂	Other oxides	PF
CP V-ARI	62.98	16.84	5.24	2.87	5.48	4.79	1.10	–	0.23	0.46	3.42
Fly ash	1.60	57.80	26.30	6.20	0.30	0.80	3.00	0.60	1.30	0.40	1.61
Other oxides: SrO + MnO + Tm ₂ O ₃ + V ₂ O ₅ + ZnO											
Fly ash—Alkaline equivalent (Na ₂ O _{equiv.} = Na ₂ O + 0.658·K ₂ O): 2.57%											
Fly ash—SiO ₂ + Al ₂ O ₃ + Fe ₂ O ₃ = 90.3%											

Table 2 X-ray fluorescence of the naturally contaminated aggregate

Sample	SiO ₂ (%)	Fe ₂ O ₃ (%)	Al ₂ O ₃ (%)	CaO (%)	TiO ₂ (%)	MgO (%)	Na ₂ O (%)	K ₂ O (%)	P ₂ O ₅ (%)	SO ₃ (%)	MnO (%)	SrO (%)	PF (%)
Contaminated sand	47.1	18.3	13.0	9.1	3.2	2.8	2.5	1.5	0.8	0.3	0.2	0.1	0.8

Table 3 Proportional contamination levels in SO₃ and pyrite

Content of SO ₃ (%)	Content of pyrite (%)
0.00	0.00
0.50	0.38
1.00	0.75
5.00	3.75

Table 4 Levels of pyrite in relation to the total mass of the aggregate of the base concrete mix proportioning and the cement mass

Series studied	Pyrite content in the total mass of aggregate (%)	Pyrite content relative to cement weight (%)
Ref. (0.0%)	0.00	0.00
SO ₃ (0.5%)	0.38	2.05
SO ₃ (1.0%)	0.75	4.05
SO ₃ (5.0%)	3.75	20.25

hydroelectric power plant, which employed the CP IV cement. The contamination rates were applied on the total mass of aggregates (2.7 kg fine aggregate + 2.7 kg coarse aggregate) and determined the proportional contamination with respect to the cement mass, as by the results shown in Table 4.

The studied cement paste was prepared with pozzolanic cement composed in a laboratory with the addition of 20.25% of limestone filler on the weight of the cementitious material (CP V cement + fly ash). The water/cement ratio used in mixing the paste was 0.6, kept constant in all studied systems.

In the contaminated cement pastes, filler limestone was gradually replaced in mass by pyrite, due to the different contamination levels, until the paste group with 3.75% of pyrite weight, had all the limestone filler replaced by the contaminant.

2.1.2 Mortars

In the mortars two different mix proportions were studied, the reference one, which had no sulphide contamination, and the group with the naturally contaminated aggregate.

In both mortar traces the proportion of 1 part cement to 3 parts sand was employed, maintaining the water/cement relation to 0.6.

As the contamination, in this case, is of natural origin, there was no addition of material, neither pyrite nor filler.

For the analysis of the results, the two mix proportions were divided into two series: 1—Natural sand: mortar with natural sand without contamination; 2—Artificial Sand: mortar with (crushed) artificial sand with natural pyrite contamination.

2.2 Testing procedures

For the strength tests to compressive and tensile strength in bending, dimensional prismatic specimens were moulded ($4 \times 4 \times 16$) cm³. For the dimensional variation test, specimens were moulded, also prismatic, but with dimensions ($2.5 \times 2.5 \times 28.5$) cm³. Furthermore, at the time of the moulding, small samples, of approximately 10 g, were collected, for the scanning electron microscopy test.

Cement pastes and mortars were mixed in a mechanical mixer, as described in the Brazilian NBR 13276 [23].

The consolidation was carried out with spatula beats and, at the end of the mould filling the top section of the paste was levelled. After 48 h, the specimens were removed from the mould and subjected to wet curing in water saturated with lime, until they were 28 days.

The compression strength and tensile strength in flexion testing was performed at 28 and 168 days to evaluate the mechanical properties of the materials. The mechanical tests were performed in accordance with the recommendations of the NBR 13279 [24]. In the first test held to evaluate the tensile strength in bending, the specimen broke up in half with the following dimensions ($4.0 \times 4.0 \times 16.0$) cm³. The load application rate for this test was (50 ± 10) N/s, using 5 specimens for each age. After the tensile test in flexion, there were 10 resulting specimens (resulting halves of the tensile test in flexion), which were subjected to an axial compression test at a loading rate of (500 ± 50) N/s.

For the dimensional variation analysis of the prismatic test specimens ($2.5 \times 2.5 \times 28.5$) cm³, measurements were performed on a standard porch with dial indicator, accurate to 0.001 mm. Readings were always held on the same side and measuring direction. Due to the sensitivity of the test, was opted for daily performance readings in the first 28 days and after that, weekly readings.

For the scanning electron microscopy, the samples underwent a preparation that followed the following methodology: (I) fragmentation of the sample into pieces

with a maximum dimension of 5.0 mm (approximately); (II) immersion of the fragmented pieces into ethyl alcohol for 24 h to stop the chemical reactions, and (III) drying the material in an oven at 40 °C [25].

Microscopy images were obtained with an FEG microscope, Tescan, Mira 3 with a coupled X-ray analytical microprobe, Oxford X-Max 50 (EDS).

Up to 28 days the samples were subjected to submerged curing saturated with lime, after which the materials were exposed to two different exposure conditions, 20 wetting and drying cycle and constantly aerated tank.

The different conditions were employed to accelerate the reactions, since there would be availability of oxygen and water. The methodology of evaluation of the process of attack by sulfates with a proposal of acceleration of the process through cycles of wetting and drying has already been used by other authors such as Gao et al. [2], Gong et al. [26], Jiang and Niu [27] and Capraro et al. [28].

The study was performed up to 168 days of age (28 days of curing + 140 days of exposure) to represent an advanced stage of the deterioration mechanism.

3 Results and discussion

3.1 Axial compressive strength and bending tensile strength of cement pastes

Figure 1 shows the compressive strength values for the four cement paste series. It was observed that the compressive strengths were close to 20 MPa, consistent with the concrete used as a reference and that it has the same water/cement relation as the pastes of this experiment. In addition, it is noted that the replacement of limestone fillers with pyrite, at 28 days, caused an increase in the strength of the cement pastes.

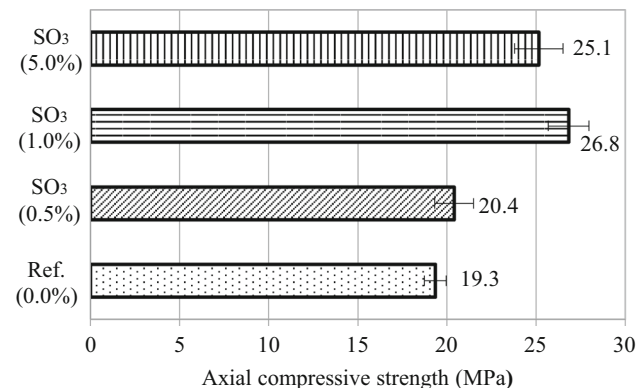


Fig. 1 Axial compressive strength in cement paste at 28 days (underwater curing condition)

Applying the Tukey test on the results obtained, with 95% confidence, a statistical equivalence was seen, but only between the Ref. (0.0%) and SO₃ (0.5%) series. At this age, then, it might be said that the series with the highest SO₃ contamination (1.0%) and (5.0%) SO₃ showed greater strength to axial compression when compared with the reference series and the series with smaller contamination. The series with the highest compressive strength at that age was the (1.0%) SO₃. The larger strength values to axial compression of the series with the highest contamination (1.0%) SO₃ and (5.0%) SO₃ can be explained by different factors.

First, these two features showed higher cement consumption (approximately 3%), because when the replacement of materials with different specific mass is done, the consumption by volume changes. This may have contributed to the fact that, at 28 days, the compressive strength was higher than the others.

Another factor that may explain the increased compressive strength, better discussed in the results of the scanning electron microscopy tests, is the filling of the pores of the cement paste, with consequential products of the internal attack sulphates. This agrees with what was exposed by Chinchon-Paya et al. [8], Araújo [9], Hoppe Filho et al. [29], Medeiros et al. [30] and Souza et al. [31], since the formation of products from the reaction between the hydrate and sulphate ions available, in the voids, fills the spaces and can promote strength gains at an early stage (up to 200 days).

After 168 days of cement paste age, the series with the greatest contamination of SO₃ (5.0%), could, by the same statistical test, be considered equivalent to the Ref. (0.0%) and (0.5%) SO₃ groups. This similarity between the group without contamination and lower contamination with the group of greater contaminations, might not indicate a decline in compressive strength of the latter, but a strength growth lower than the others.

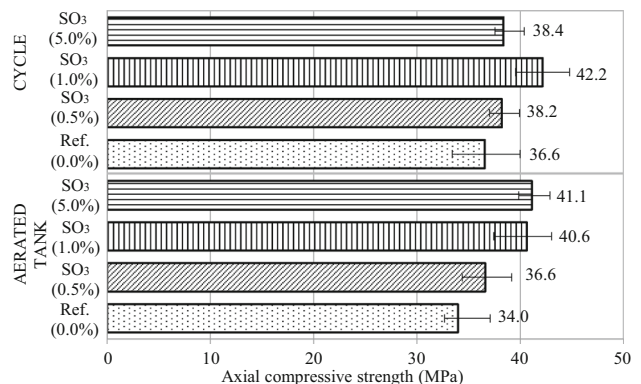


Fig. 2 Axial compressive strength of the cement pastes at 168 days (28 days in submerged cure + 140 days of exposure)

The delay in strength gain observed in the (5.0%) SO₃ series agrees with the results obtained by Pereira [22] and Oliveira [32]. It is thereby assumed that the sulphate made available by the early reactions of pyrite oxidation changed the cement hydration kinetics, showing differences in compressive strength at 168 days. The strengths values obtained at this age are shown in Fig. 2.

Regarding the exposure conditions employed, no different statistics were found for the same Tukey test. It was observed that the series were considered statistically equivalent between them, except for SO₃ (5.0%), which presented higher compressive strength (41.1 MPa) in the cycle condition than in the aerated tank condition (38.4 MPa), the latter indicating the worst exposure condition in this case.

The results of bending tensile strength at 28 days (Fig. 3) did not allow any distinction between sets, all being considered statistically equivalent Tukey test, with 95% confidence.

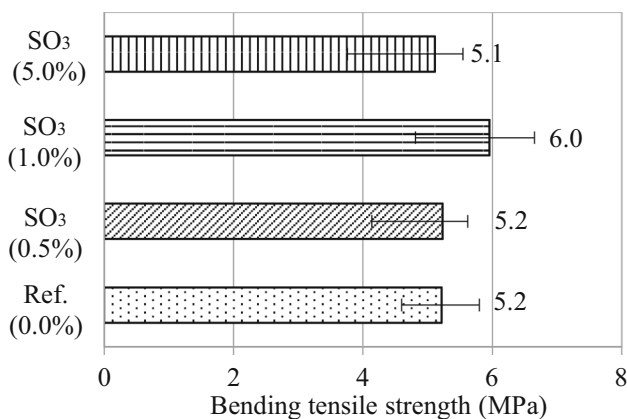


Fig. 3 Bending tensile strength of the cement pastes at 28 days (submerged curing condition)

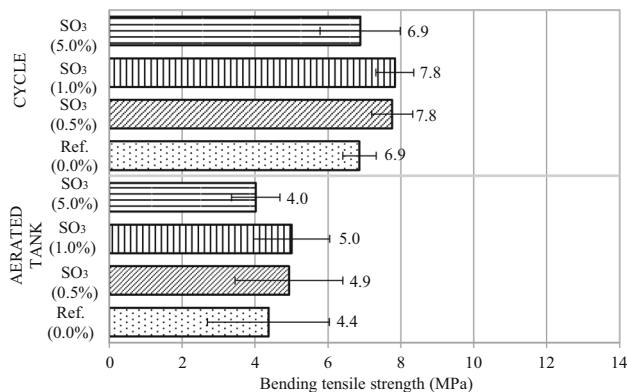


Fig. 4 Bending tensile strength of the cement pastes at 168 days (28 days submerged cure + 140 days of exposure)

The results, at 168 days, again showed no significant difference between the studied series, and, until this age, materials of the same tensile strength in flexion. Figure 4 shows the results obtained at that age. For the exposure conditions, it was noticed that at 168 days, the condition of the wetting and drying cycle was the worst for all the series, showing significant difference when compared to themselves. This can be explained by the volume variations, that occurred in the material due to alternating expansion conditions (wetting) and retraction (drying). This change would increase the micro cracks forming inside the specimens, lowering its tensile strength, going against what was exposed by Vieira and Dal Molin (2011) [33].

3.2 Axial compressive strength and bending tensile strength of mortars

In Fig. 5 are shown the compression strength values for the mortar at 28 days. Analysing the results at 28 days, a greater strength was observed in series with artificial aggregates, indicating the same trend as occurred with the cement pastes.

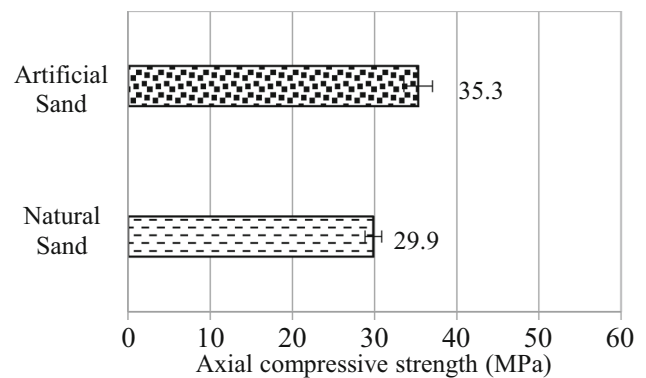


Fig. 5 Axial compressive strength of mortars at 28 days (underwater curing condition)

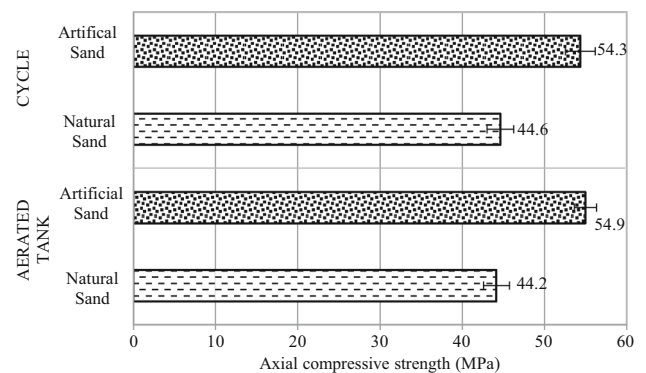


Fig. 6 Axial compressive strength of mortars at 168 days (28 days submerged cure + 140 days of exposure)

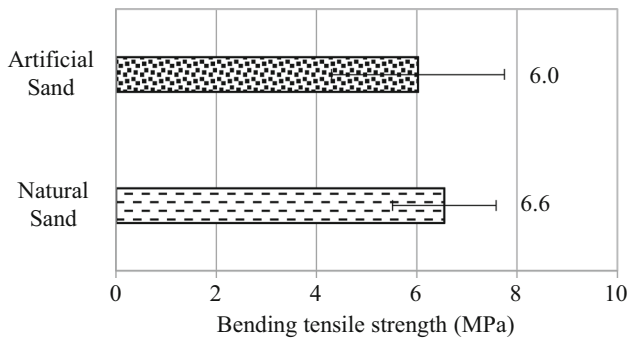


Fig. 7 Bending tensile strength of mortars at 28 days (submerged healing condition)

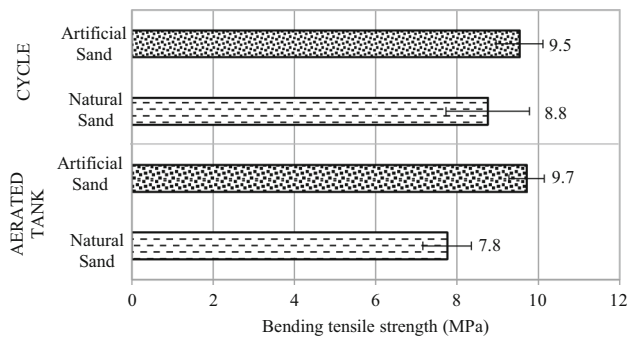


Fig. 8 Bending tensile strength of mortar at 168 days (28 days submerged cure + 140 days of exposure)

At 168 days, the difference between the groups remained high, with contaminated mortar being more strength. Figure 6 shows the results obtain at that age.

Corroborating with the results obtained in the test of axial compression strength of the cement pastes, at

168 days, no significant difference between the exposure conditions by the Tukey test were noticed. The behaviour of mortars in the flexion tensile test was like those presented in pastes, or at 28 days the two groups were statistically equivalent (Fig. 7).

At 168 days, there was a change of behaviour, and on the wetting cycle condition and drying the groups might be considered significantly different, with the contaminated mortar as the strongest. Figure 8 shows the results obtained at that age.

Contrary to what occurred with the cement pastes, there was no consensus in the mortar on the most harmful condition. The natural sand mortar, at 168 days, had greater strength in the aerated tank condition, while the mortar with artificial sand, presented statistically equivalent results in both conditions studied.

3.3 Dimensional variation of cement paste bars

In Fig. 9 the dimensional variety of the cement pastes is represented, when subjected to weekly cycles of drying and wetting.

The reference cement paste, which contains limestone fillers in its composition, presented the biggest retraction among the studied pastes. The retraction occurred gradually until 11 days, at which stabilizes and starts to fluctuate due to the type of exposure to which it is submitted. The partial replacement of limestone fillers for pyrite, at different levels, has reduced the retraction as high as the pyrite content that used in the composition of the pastes. The use of material contaminated in 1.0% SO₃ content reduced the retraction to approximately half of the decline observed in the reference paste. With 5.0% SO₃ content

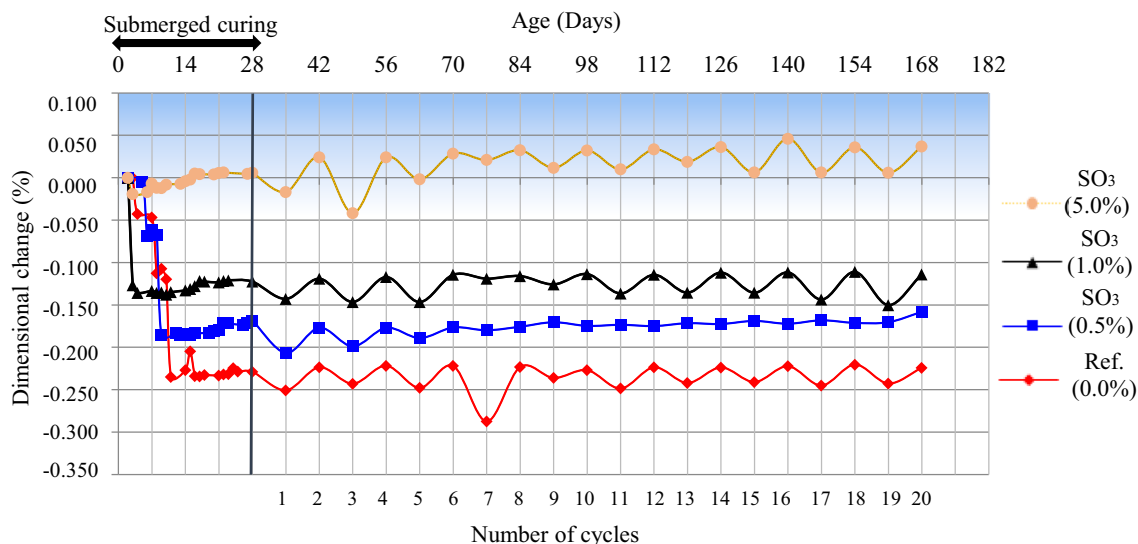


Fig. 9 Dimensional variation of the test specimens subjected to the wetting and drying cycle at 168 days

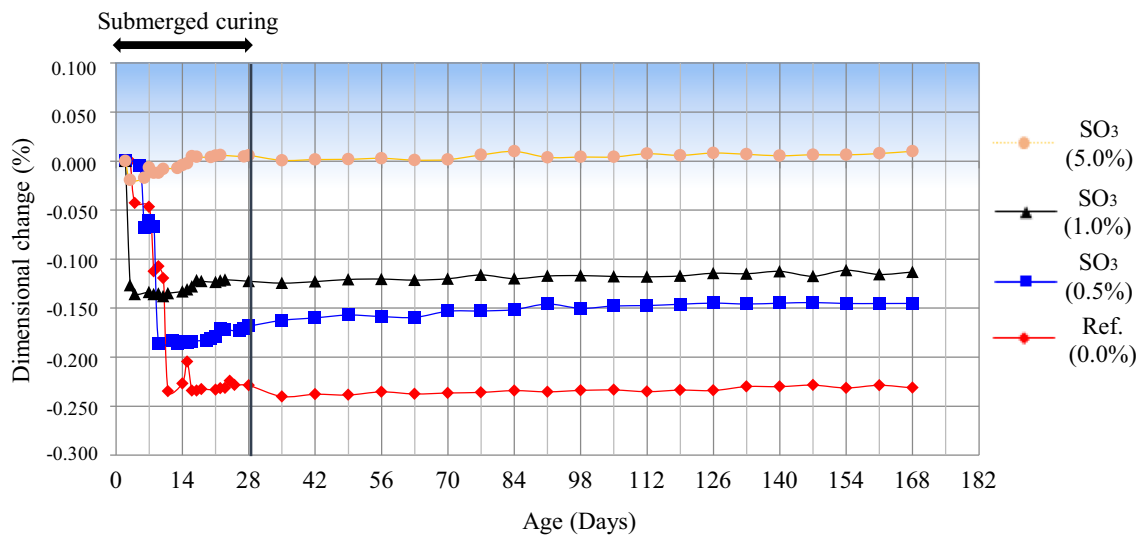


Fig. 10 Dimensional variation of the specimens submitted to the aerated tank at 168 days

there was practically no dimensional change at 28 days, until prior to the exposure to drying and wetting cycles. This behaviour is an indication that there is a beginning of pyrite oxidation and formation of expansive hydrated compounds, in other words the formation of expansive compounds is influencing and acting as reducing the retraction. From 28 days, exposure to drying and wetting cycles led to dimensional changes (retraction/expansion) of the paste, which on average, were like the size observed at 28 days, just before wetting procedures and drying. This behaviour indicated that up to 168 days, the pyrite oxidation reaction was not significantly influenced by varying the exposure condition, which aimed to provide water and oxygen for its occurrence.

Figure 10 shows the dimensional variation of the bars exposed to the aerated tank. The behaviour up to 28 days was

like that of the samples submitted to the cycle; after all, until that age all were in cure. Unlike those submitted to the cycle, after 28 days, no considerable dimensional variation was noticed in the bars submitted to the aerated tank.

3.4 Dimensional variation of the mortar bars

Mortar showed smaller dimensional variations than presented by the cement paste. This difference in behaviour follows the filling consumption of the cement used, since the cement pastes have a higher consumption of cement per m³ of the mortar. The greatest change observed in the pastes was close to -0.3% (Fig. 9) while the mortar most variation was -0.044% (Fig. 11) to the both reference series. However, the behaviour trend was like that presented by pastes, in other words the reference group

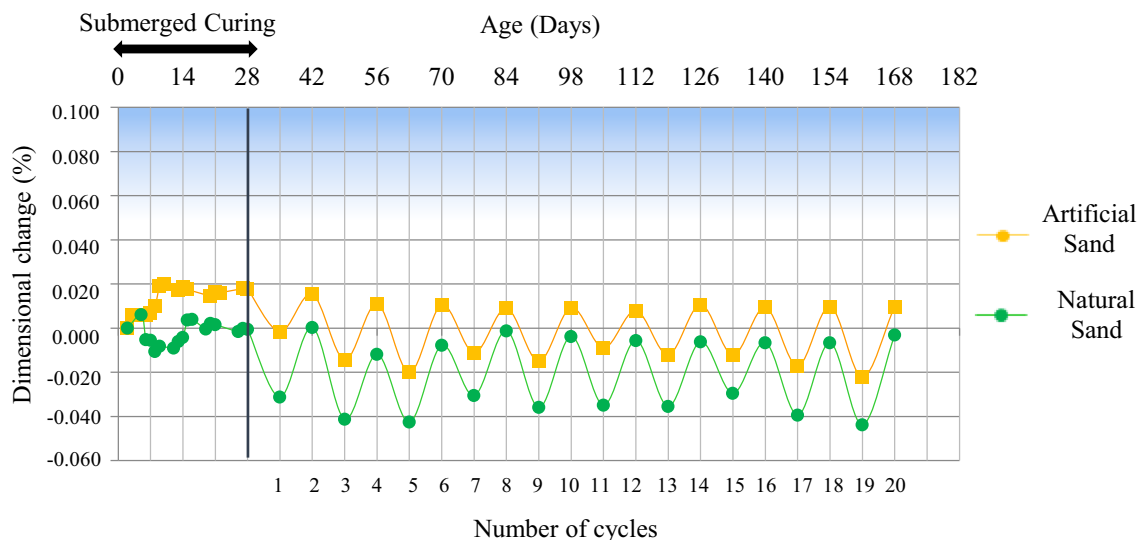


Fig. 11 Dimensional variation of the specimens of mortar subjected to wetting and drying cycle at 168 days

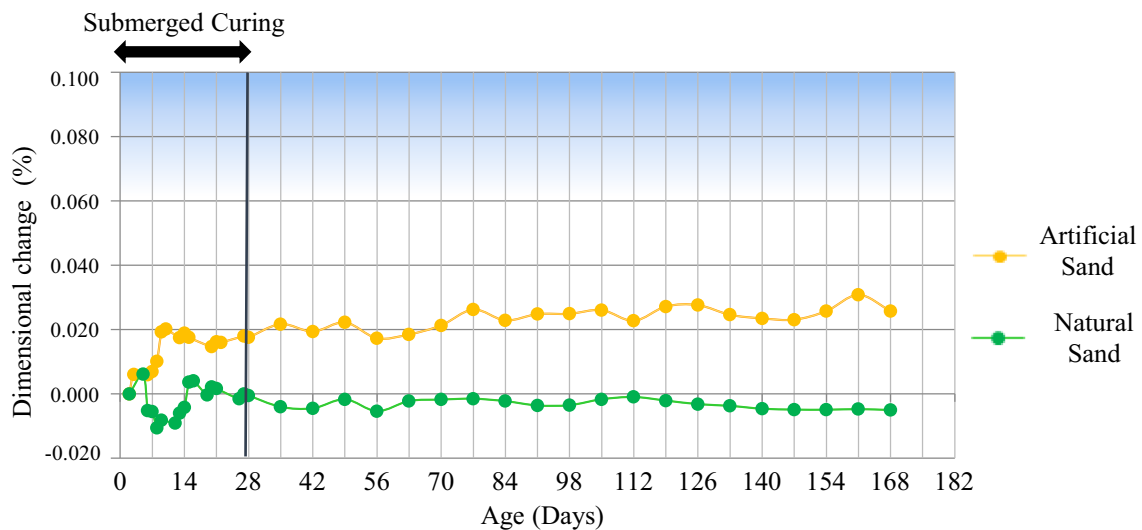


Fig. 12 Dimensional variation of the mortar specimens subjected to the aerated tank at 168 days

(natural sand), in the early days showed a dimensional change due to the initial retraction. This occurred to a lesser extent, and only by the 8th day old material. Figure 11 shows the results for the dimensional change of the bars exposed to the wetting and drying cycle. Note the oscillating values after 28 days, resulting in alternating immersion conditions of wetting and dry chamber.

In samples exposed to the aerated tank (Fig. 12) we observed an almost constant behaviour, with little fluctuation after the initial hydration period and extending to 168 days. It should be noted that in both exposure to immersion in aerated tank, as in the case of wetting and drying cycle, the results up to 168 days indicate expansion

for the artificial sand and retraction for the natural sand (the reference number).

3.5 Electron microscopy scanning with EDS in cement pastes and mortar

The micrographs and the result of elemental analysis by EDS enabled to identify acicular crystals similar to those of ettringite product derived of internal attack of the sulphates, both in higher contamination of pastes series SO₃ (1.0%) and SO₃ (5.0%), as in the contaminated lot of mortar already after 28 days.

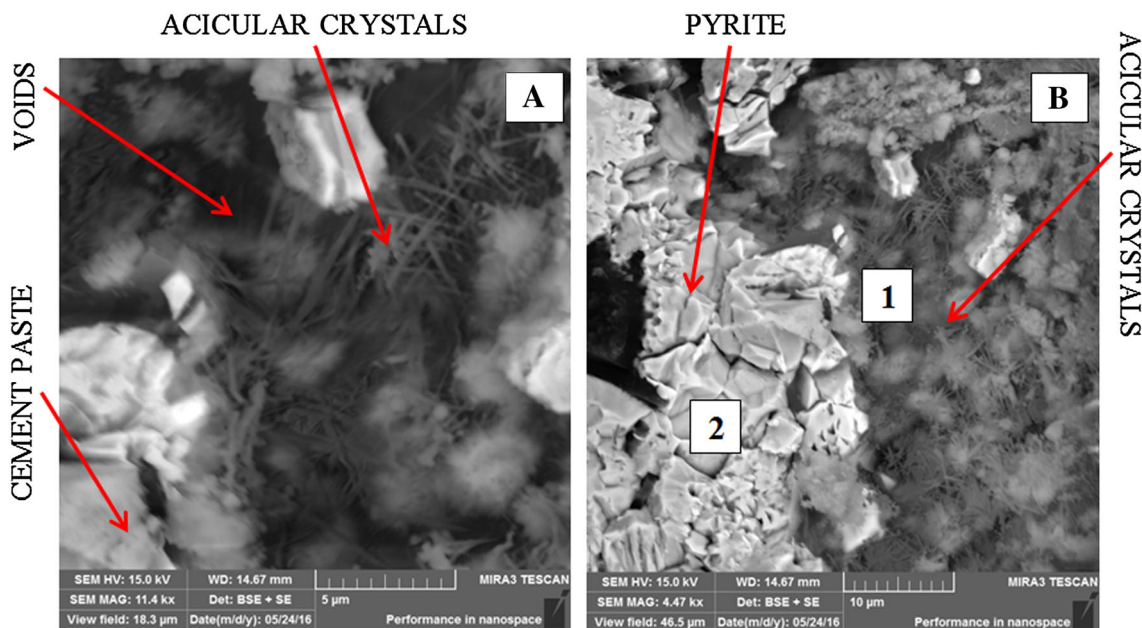


Fig. 13 Electron microscopy scanning obtained for SO₃ series (5.0%) of the pastes at 28 days (submerged curing condition)

In the cement pastes, the crystals were identified mainly in empty voids and available around the pyrite grains, as shown in Fig. 13a and b, respectively. The filling of the voids help corroborated with the results obtained in the axial compression test of pastes, for the formation of crystals in these spaces allow a greater compactness of the material, causing it to resist to increased efforts.

In elemental analysis was noted the presence of iron and sulphur in the region corresponding to the presence of pyrite (region 1 in Fig. 13b) and of calcium, aluminium and sulphur in the region where there is dispersion of crystals with a morphology of needles (region 2 of Fig. 13b). In Figs. 14 and 15 shows the spectra obtained for the two regions.

Analysing the theoretical stoichiometric ratio of the elements, with the content of basic compounds by EDS (Table 5), little difference was noted in the percentages obtained from analysis. Comparing the percentages, there has been a reduction in the sulphur element, which led to understanding that it may have some chemical process of releasing the element and fixing it in another compound.

Making a similar analysis to the previous one, we realized the similarity between the theoretical proportions of ettringite and content of basic compounds by EDS (Table 6). Even if the values are slightly different, this does

Table 5 Proportion of iron and sulphur in pyrite elements

Elements	Percentage of theoretical elements in pyrite (%)	EDS (%)	Normalization EDS (pyrite) (%)	Difference (%)
Fe	46.55	52.10	33.92	12.63
S	53.45	39.80	39.80	0.00

Table 6 Percentage of the elements calcium, aluminium, sulphur, oxygen and hydrogen in the ettringite

Elements	Percentage of theoretical elements in ettringite (%)	EDS (%)	Normalization EDS (ettringite) (%)	Difference (%)
Ca	19.13	23.30	12.50	10.80
Al	4.30	2.80	2.80	0.00
S	7.67	5.70	5.00	0.70
O	63.74	50.10	41.50	8.60
H	5.14	–	–	–

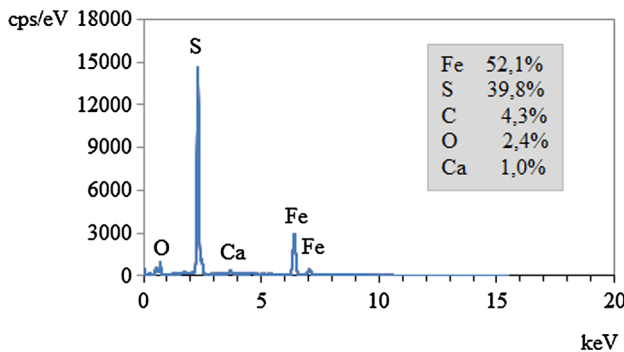


Fig. 14 EDS spectrum obtained for the region 1 in Fig. 13b

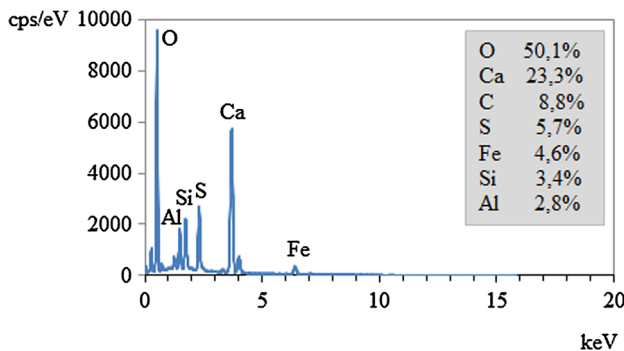


Fig. 15 EDS spectrum obtained for region 2 of Fig. 13b

ACICULAR CRYSTALS PORTLANDITE



Fig. 16 Electron microscopy scanning obtained for contaminated series of mortars at 28 days (submerged healing condition)

not misinterpret the presence of ettringite but indicates the presence of this crystal and some other compound together. This may be a result of an EDS-based edge effect, since the beam is directed to a point. The capture of electrons can also be made in nearby regions, offering the possibility of reflections to other compounds.

In the series of mortar with sand contaminated by sulphides, we noted in the same crystals with acicular needles morphology in the surroundings of hexagonal plates,

similar to portlandite. Figure 16 presents the image obtained for the contaminated group of mortars at 28 days.

4 Conclusions

The results of all tests used in this study helped in the process of understanding the degradation mechanism of the internal attack by sulphates. It was noticed that there are many variables involved and the occurrence time of attack is a decisive factor.

The analysis of the mechanical properties by compressive strength and bending tensile strength indicated in the study period that the contaminated materials showed better results than the references, according to reports by other authors [6–8]. This increased strength can be better understood with the images obtained by scanning electron microscopy, since, at 28 days, needle-like crystals were identified scattered in the cement pastes and empty spaces of materials, indicating the filling of these spaces. As there was no decrease in the mechanical strength and there was the appearance of visible cracks in the faces of the samples, it is possible to conclude that the pores in the cement pastes and mortars were not completely filled to the point that the reactions resulting from the attack caused internal tensions. In this way, it was observed that, at the period of 168 days and with the exposure conditions adopted, the contaminated samples don't present any damage to the mechanical properties, being this initial stage of the attack.

The dimensional change in bar behaviour indicated a difference already at the early stages, and the group SO₃ (5.0%), the one with the greatest contaminant addition, was responsible for the greatest expansion obtained.

In summary, the overall evaluation of the results showed that probably the attack process by internal sulphates are in the initial stage, with increased mechanical strength and expansion without the emergence of still visually apparent cracks.

Acknowledgements The authors thank the infrastructure and support in human resources and funding to COPEL GeT project R&D 6491-0301/2013, to ANEEL, and Coordenação de Aperfeiçoamento de Pessoal de Nível Superior (CAPES), Fundação Araucária, LAC-TEC institute, to CNPq Lei 8010/90 (LI 15/2187214-1; LI 14/4695814-5; LI14/3410726-9) and the Federal University of Paraná (PPGECC/UFPR)—Brazil.

References

- Duchesne J, Fournier B (2013) Deterioration of concrete by the oxidation of sulphide minerals in the aggregate. *J Civil Eng Archit* 7(8):922–931
- Gao J, Yu Z, Song L, Wang T, Wei S (2013) Durability of concrete exposed to sulfate attack under flexural loading and drying–wetting cycles. *Constr Build Mater* 39:33–38
- Ikumi T, Segura I, Cavalaro SHP (2017) Influence of early sulfate exposure on the pore network development of mortars. *Constr Build Mater* 143:33–47
- Centurione SL, Kihara Y, Battagin AF Durability of concrete subjected to sulfate ion attacks. In: *Annals of the 47th Brazilian Congress of Ceramics*. João Pessoa, 2003
- Coutinho JS (2001) Sulphate attack. Faculty of Engineering of Porto (FEUP). Portugal
- Pereira E, Bragança MOGP, Oliveira IC, Godke B, Portella KF (2014) Internal sulfate attack on pyrite contaminated concrete structures: a literature review. 1st Brazilian Congress of Construction Pathologies. Paraná
- Gomides MJ (2009) Investigation of aggregates containing sulfides and their effects on the durability of concrete. Doctoral Thesis, Federal University of Rio Grande do Sul. Porto Alegre
- Chinchón-Payá S, Aguado A, Chinchón S (2012) A comparative investigation of the degradation of pyrite and pyrrhotite under simulated laboratory conditions. *Eng Geol* 127:75–80
- Araújo GS (2008) La reacción sulfática de origen interno em presas de hormigón. Propuesta metodológica de análisis. Tesis Doctoral Universitat Politècnica de Catalunya. Departament d'Enginyeria de la Construcción. Barcelona
- Prado PF, Soares AB, Souza VP, Soares PSM (2011) Determination of the intrinsic oxidation rate of pyrite in coal tailings. *Brazilian Congress of Mineral Coal*, Gramado
- Casanova I, Aguado A, Agulló L, Vázquez E (1996) Physico-chemical analysis of expansive phenomena in concrete dams. *Dam Eng* 07:249–270
- Aguado A, Agulló L, Cánovas MF, Salla JM (1996) Diagnóstico de daños y reparación de obras hidráulicas de hormigón. Colegio de Ingenieros de Caminos, Canales y Puertos, Madrid
- Oliveira I, Cavalaro SHP, Aguado A (2013) New kinetic model to quantify the internal sulfate attack in concrete. *Cem Concr Res* 43:95–104
- Hasparyk NP, Muniz FC, Andrade MAS, Gomides MJ, Bittencourt RM, Carasek H (2003) The deterioration of concrete structures containing aggregates with sulphides. In: *Epusp symposium on concrete structures*
- Goto H, Braga VS, Capraro APB, Medeiros MHF, Bragança MOGP, Portella KF, Oliveira IC (2016) Physicochemical evaluation of oxidation of diabase aggregates with sulfide minerals: influence of particle size, pH of the medium and pyrite concentration. *J Build Pathol Rehabil* 1:8
- CEMIG (2007) Behavior of concretes and injection boils in the presence of sulphated rocks. Research project P&E0122. UHE Irapé
- ASSOCIATION FRANÇAISE DE NORMALISATION. AFNOR NF P 18-540. Granulats—Définitions, conformité, spécifications. Paris, 1997
- ASSOCIAÇÃO BRASILEIRA DE NORMAS TÉCNICAS. NBR 7211: Concrete aggregates—Definitions. Rio de Janeiro, 2009
- American Concrete Institute. Guide to Durable Concrete. Detroit—USA, 1991. (ACI 201)
- ASSOCIAÇÃO BRASILEIRA DE NORMAS TÉCNICAS. NBR 5736: Pozolanic Portland Cement. Rio de Janeiro, 1999
- ASSOCIAÇÃO BRASILEIRA DE NORMAS TÉCNICAS. NBR NM 248: Aggregates—determination of the granulometric composition. Rio de Janeiro, 2003
- Pereira E (2015) Investigation and monitoring of internal sulfate attack on concretes in early ages. Doctoral Thesis, Federal University of Paraná. Curitiba
- ASSOCIAÇÃO BRASILEIRA DE NORMAS TÉCNICAS. NBR 13276: Mortar for laying and coating of walls and ceilings—preparation of the mixture and determination of the consistency index. Rio de Janeiro, 2005

24. ASSOCIAÇÃO BRASILEIRA DE NORMAS TÉCNICAS. NBR 13279: Mortar for laying and coating of walls and ceilings—determination of tensile strength in bending and compression. Rio de Janeiro, 2005
25. Pan Z, Li D, Yu J, Yang N (2002) Hydration products of alkali-activated slag-red mud cementitious material. *Cem Concr Res* 32:357–362
26. Gong J, Cao J, Wang Y (2016) Effects of sulfate attack and dry-wet circulation on creep of fly-ash slag concrete. *Constr Build Mater* 125(30):12–20
27. Jiang L, Niu D (2016) Study of deterioration of concrete exposed to different types of sulfate solutions under drying-wetting cycles. *Constr Build Mater* 117(1):88–98
28. Capraro APB, Medeiros MHF, Hoppe Filho J, Bragança MOGP, Portella KF, Oliveira IC (2017) Internal sulfate reaction (ISR) as degradation of the cement matrix: behavior of pastes dosed with different amounts of contamination by sulfate. *Rev ALCONPAT* 7:119–134
29. Hoppe Filho J, Souza DJ, Medeiros MHF, Pereira E, Portella KF (2015) Concrete attack by sodium sulfate: mineral additions as a mitigation tool. *Cerâmica* 61:168–177
30. Medeiros MHF, Souza DJ, Hoppe Filho J, Adorno CS, Quarcioni VA, Pereira E (2016) Red-clay waste and limestone filler added in Portland cement composite: effects on sulfate attack and alkali-silica reaction. *Matéria (UFRJ) JCR* 21:282–300
31. Souza DJ, Yamashita LY, Dranka F, Medeiros MHF, Medeiros Junior RA (2017) Mortars incorporating multi-walled carbon nanotubes: shrinkage and sodium sulphate attack. *J Mater Civil Eng JCR (NO PRELO)*
32. Oliveira IC (2013) Data analysis for the elaboration of guidelines for the detection of sulfides and sulphates in the CCR composition. Masters Dissertation, Federal University of Paraná. Curitiba
33. Vieira GL, Dal Molin DCC (2011) Evaluation of compressive strength, tensile strength and micro cracking formation in concretes produced with different cements, when a preloading of compression is applied. *Ambiente Construído*. Vol. 11 n 1. Porto Alegre